Thermochimica Acta, 152 (1989) 165–173
Elsevier Science Publishers B.V., Amsterdam — Printed in The Netherlands

DYNAMIC SURFACE-TENSION MEASUREMENTS ON SURFACE-ACTIVE MATERIALS: PART II

A.A.H.Boonman[1], P.M.C. Gieles[2], C.H.Massen[3], J.Egberts*
Department of Physics, Eindhoven University of Technology,
P.O.Box 513, 5600 MB Eindhoven, The Netherlands.
*Department of Obstetrics and Gynaecology, Leiden University
Medical Centre, 2333 AA Leiden, The Netherlands.
[1]Netherlands Asthma Fund, [2] Foundation for Biophysics, [3]Letters should be addressed to this author.

SUMMARY

Further research is presented on a modification of the Langmuir-Wilhelmy technique, the asymmetric method, for quick measurement of the surface-dilational elasticity ϵ_d in relation to the surface pressure π. Assessment of the dynamic response of the electrobalance shows that first-order transfer can be assumed. A method is described of calculating the modulus and loss angle of ϵ_d under both uniform and nonuniform conditions. Measurements of the ϵ_d–π relation have been performed on phospholipids from purified lung surfactant of foetal sheep in relation to foetal age in the last period of gestation. No significant variations of $|\epsilon_d|$ and ϕ_ϵ with foetal age have been found.

INTRODUCTION

In our first paper on this subject (ref.1) we discussed the use of an automatic balance provided with a Wilhelmy plate for surface-tension measurements. We described a modification of the Langmuir-Wilhelmy technique for application to surface-rheological measurements. Normally, the Langmuir-Wilhelmy technique makes use of a hydrophobic trough filled with a liquid and a hydrophobic barrier to vary the air-liquid interface. For our purpose, the trough has been equipped with a second barrier (Fig. 1). This second barrier generates small harmonic variations (δA) in area (A) of an air-water interface. The first barrier is used for setting the interface area. This modified technique will be referred to as the asymmetric method.

In the case of an interface covered with an insoluble monolayer, the variations in area will result in harmonic variations ($\delta\sigma$) of the surface tension (σ). If the automatic balance responds fast enough, the variations in surface tension can be measured. In our previous paper (ref.1) we defined a complex transfer function ϵ_d by

0040-6031/89/$03.50

$$d\sigma = \epsilon_d \, d\ln A \qquad (1)$$

where $d\ln A = dA/A$ and $d\sigma$ and dA are infinitesimal variations of σ and A.

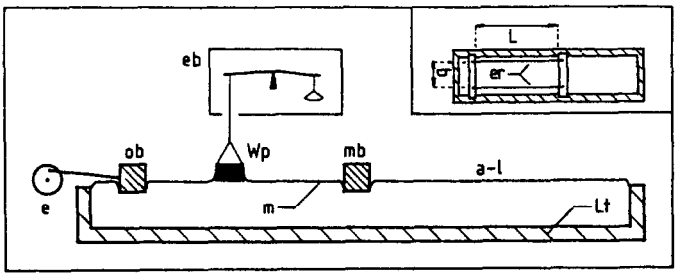

Fig. 1. Principle of the apparatus of the asymmetric method. The insert shows a top view. Abbreviations: eb, electrobalance; Wp, Wilhelmy plate; Lt, Langmuir trough; mb, moving barrier; ob, oscillating barrier; e, excenter; a-l, air-liquid interface; m, monolayer; L and b, length and width of monolayer area; er, elastic ribbon.

and dA is assumed to be dilational. ϵ_d is called the surface dilational-elasticity, and can be written as

$$\epsilon_d = |\epsilon_d| e^{j\phi_\epsilon} \qquad (2)$$

where $|\epsilon_d|$ is the modulus and ϕ_ϵ the loss angle of ϵ_d. We presented $|\epsilon_d|$ values from measurements on monolayers of synthetic phospholipids. In the paper we will present further research on the method and results of measurements. First, the behaviour of the electrobalance used was investigated in greater detail. Second, we describe a more general method of calculating ϵ_d than that used in our previous paper. Third, results of measurements on monolayers of phospholipids extracted from lung surfactant of sheep foetus will be presented. These values of ϵ_d have been measured in relation to foetal age in order to investigate the relation between ϵ_d and foetal maturation.

DYNAMIC BALANCE TRANSFER

Method

The transfer of a harmonically time-dependent force was measured by means of a set up (ref. 2) as outlined in Fig. 2. A cylindrical permanent magnet PM was suspended from the balance and located near a coil (L=4.67H). A sinus generator was used to generate a sinusoidally time-dependent field (angular frequency ω) in the coil. The magnet was arranged in such a way that it was

exposed to an inhomogeneous but axially symmetrical field of the coil. The voltage drop V_i over the resistor R (R≈10 Ohm) and the signal V_o of the control unit CU of the balance were fed to a micro computer via a double channel filter. The forces acting on the electrobalance, being a static one arising from the mass of the magnet (≃0.9g) and a varying one caused by the field of the coil have been chosen in the same order of magnitude as those prevailing during the dynamic surface-tension measurements. The field of the coil did not influence the electrobalance. Assuming a first-order transfer $B(\omega)$ between V_i and V_o, the modulus $|B|$ and the phase angle ϕ_B read

$$|B| = \frac{|B(0)|}{\sqrt{(1 + (\omega t_B)^2)}} \qquad (3)$$

$$\phi_B = -\arctan(\omega t_B) \qquad (4)$$

where t_B is a time constant.

Results

Fig. 3 shows the measured values of $|B(0)|/|B|$ versus ω^2 and of $\tan(\phi_B)$ versus ω. The plots are straight lines as is to be expected according to eqns. (3) and (4), and thus a first-order transfer is a good approximation. Application of eqn. (3) yields t_B=0.106±.02s, while that of (4) leads to t_B=0.103±.02s.

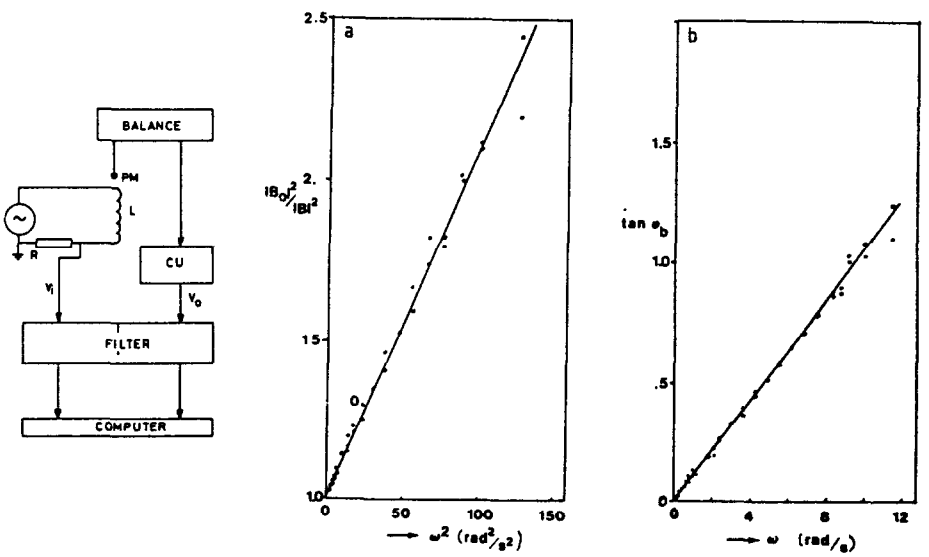

Fig. 2. (left) Principle of the determination of the balance transfer see text.
Fig. 3. Response of the electrobalance. Fig. 3a (middle) $|B(0)|^2/|B|^2$ vs ω^2. Fig. 3b (right) $\tan(\phi_B)$ vs ω.

We accounted for the dynamic behaviour of the electrobalance by assuming t_B=0.105s in the calculations of ϵ_s.

CALCULATION OF ϵ_d

In the previous paper (ref.1) we calculated $|\epsilon_d|$ according to

$$|\epsilon_d| = A_e \frac{\Delta\sigma}{\Delta a} \tag{5}$$

where $\Delta\sigma$ and ΔA are the amplitudes of the harmonic variations of σ and A, respectively and A_e is the equilibrium area. Eqn. (5) yields approximate values of $|\epsilon_d|$ under certain conditions (ref.3), including some correlated with a high ϵ_d (see page 5). However, the calculated values of $|\epsilon_d|$ did not allow application of eqn. (5) at all values of σ, as was found after calculation (ref.1). In order to obtain correct values, a general method of calculating $|\epsilon_d|$ and ϕ_ϵ will be described below.

In general, the variations in monolayer area generated by the oscillating barrier and propagate as a damped surface wave. When ϵ_d is high enough, only the longitudinal component of the wave is important. The information about propagation and damping of this wave is contained in the complex dispersion relation (ref.4). For $|\epsilon_d|$ and ϕ_ϵ it follows:

$$|\epsilon_d| = \frac{\sqrt{(\omega^3 \eta_1 \rho_1)}}{\kappa^2 + \beta^2} \tag{6}$$

$$\phi_\epsilon = 2 \arctan(\frac{\beta}{\kappa}) - \frac{\pi}{4} \tag{7}$$

with ω the angular frequency, η_1 the viscosity and ρ_1 the density of the liquid, κ the real wave number and β the damping coefficient. In the derivation of eqns. (6) and (7) it has been assumed that the barrier oscillates with constant angular frequency ω. Thus (6) and (7) correspond to a stationary surface wave (ref.4) and the variation in surface tension is a function of the distance x from the barrier. Taking $\delta\sigma(x)$ a sufficiently small surface-tension variation, we can write

$$\delta\sigma(x) = \Delta\sigma(x) e^{j\phi_\sigma(x)} \tag{8}$$

where $\Delta\sigma(x)$ and $\phi_\sigma(x)$ are the amplitude and the phase angle respectively. They are given by Snik (ref.3)

$$\Delta\sigma(x) = \Delta u_b |\epsilon_d| \sqrt{(\kappa^2+\beta^2)} \left[\frac{\cosh 2\beta(x-L) + \cos 2\kappa(x-L)}{\cosh(2\beta L) - \cos(2\kappa L)}\right]^{1/2} \tag{9}$$

$$\begin{aligned}\phi_\sigma(x) = \phi_b - 3\pi/4 + \arctan(\beta/\kappa) - \arctan[\tan(\kappa L).\coth(\beta L)] \\ + \arctan[\tan\{\kappa(x-L)\}.\tanh\{\beta(x-L)\}]\end{aligned} \tag{10}$$

where Δu_b and ϕ_b stand for the amplitude and the phase of the oscillating barrier. If $\Delta\sigma(x)$ and $\phi_\sigma(x)$ are measured at a given value of x, four unkown quantities $|\epsilon_d|$, ϕ_ϵ, κ and β remain in the four equations (6), (7), (9) and (10). As a result, we can calculate $|\epsilon_d|$ and ϕ_ϵ at a given value of σ_e.

A special case occurs when

(i) the troughlength L is small (L~0.1m),

(ii) the surface-dilational elasticity is so high that $\lambda >> L$ ($\lambda = 2\pi/\kappa$) and

(iii) damping is slight.

In this case, the wave character of the area deformations almost vanishes by virtue of the interference due to the multiple reflections of the wave, as mentioned by Lucassen et al. (ref.5). Since $\kappa=2\pi/\lambda$, the conditions required for this special case to occur can be written as

$$L\sqrt{(\kappa^2 + \beta^2)} << 1 \qquad (11)$$

It can be shown that eqn. (9) simplifies to eqn. (5) when the inequality (11) is valid (ref.3). From eqn. (5) it can be seen that $\Delta\sigma(x)$ and $\phi_\sigma(x)$ become independent of x. Consequently, the surface tension variation is uniform over the surface area.

As was mentioned earlier in general terms, the conditions under which (eqn. (11)) is valid were not met at all values of σ. To cope with this problem, a numerical procedure has been developed to calculate $|\epsilon_d|$ and ϕ_ϵ using eqns. (6), (7), (9) and (10).

In a different approach, eqn. (5) can be used satisfactorily. When σ is measured at x=0.43L, errors due to nonuniformity are minimal (refs. 5-6). In the asymmetric method however, this requires the adjustment of the balance position at each value of A_e. Such a procedure is however unfavourable in measurements requiring control of temperature and humidity in a climate box. Therefore a set-up was made in which the balance position is automatically adjusted after setting A_e. Reports on results of measurements are in preperation.

MEASUREMENTS ON SURFACTANT OF FOETAL SHEEP

Introduction

Variation of the composition and a number of surface properties of foetal lung surfactants towards the end of gestation has been reported in the case of several species (refs. 7-12). As regards surface-rheological properties, Snik et al. (ref. 13) measured a decrease in the surface-dilational elasticity and viscosity of foetal sheep surfactant after days 133 and 134 of gestation. This change agreed with results obtained from analysis of the composition of the surfactant. However, changes in composition with foetal

age have been found to vanish after further purification of the surfactant (ref. 14). To investigate the influence of additional purification on the rheological properties, we measured $|\epsilon_d|$ and ϕ_ϵ of the phospholipid fraction of highly purified foetal sheep surfactant in relation to foetal age.

Methods and material

The collection and purification of the foetal surfactant, the extraction of the phospholipid fraction and its composition have all been described by Egberts et al. (ref. 14). The surface-chemical apparatus and method have been described in our previous paper (ref. 1). In pilot experiments triple-distilled water was used as the subphase for comparison with the standard subphase, the latter containing Na^+, K^+, Ca^{2+}, Mg^{2+}, HCO_3^- and HPO_2^- in biologically relevant quantities. In other pilot experiments, more than one compression-expansion cycle was carried out before measurement of ϵ_d.

Results

Fig. 4 shows a plot of surface pressure π vs A, where $\pi=\sigma_0-\sigma$ and σ_0 the surface tension of pure water. This plot is obtained from the phospholipid

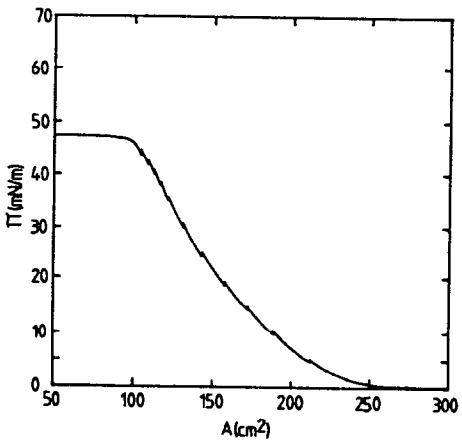

Fig. 4. π-A plot of phospholipid fraction of purified lung surfactant of sheep foetus at the 136th day of gestation (term at 142th day). 38,5°C, RH > 90% subphase containing ions (see text). First compression, compression rate: 0.5mm/s. The vertical parts in the plot are due to relaxation to constant π at constant area A_e preceeding the measurement of ϵ_d.

fraction of foetal sheep surfactant of the 136th day of gestation. This result is typical of the period investigated. We note that a transition from the liquid-expanded ('fluid') to the liquid-condensed ('solid') phase is not found. Moreover, the maximum surface pressure (π_{max}) under continued compression is only $48mNm^{-1}$. Hence, this π-A plot shows better agreement with the π-A plot of the mixed DPPC-DOPC monolayer given in the previous paper (ref. 1) than with that of pure DPPC. The value of π_{max} was $48\pm1mNm^{-1}$ over the gestational period investigated. Pilot experiments using the

cycles were applied, did not yield significantly different values of π_{max}.

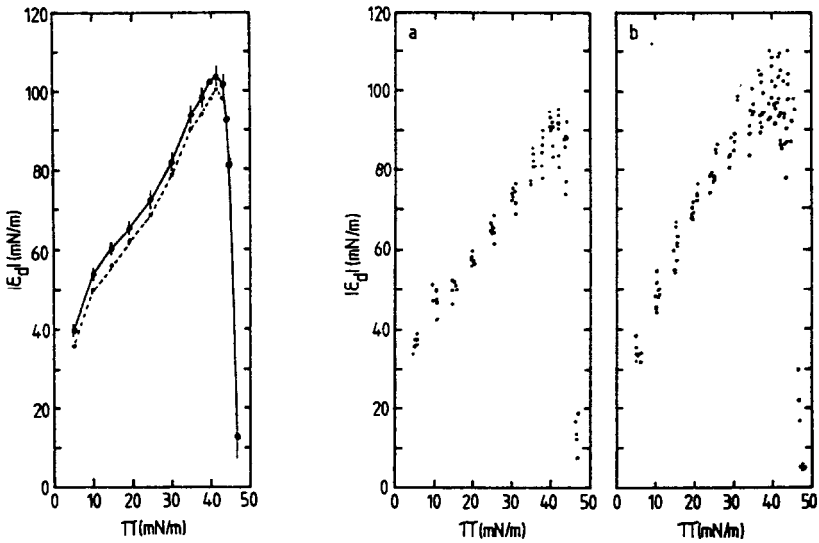

Fig. 5. (left) $|\epsilon_d|$-π plot, surfactant from 136th day, for details see Fig. 4. Broken line: $|\epsilon_d|$ calculated with eqn. (5). Solid line: $|\epsilon_d|$ calculated with eqns. (6), (7), (9) and (10). The points represent means of measurements in duplicate on two monolayers and the vertical bars the range between minimum and maximum values of $|\epsilon_d|$.

Fig. 6. Plots of single measured values of $|\epsilon_d|$ vs π, calculated with eqns. (6), (7), (9) and (10). Fig. 6.a (middle): days 130-134; Fig. 6.b: (right) days 137-140. Same details as in Fig. 4.

Fig. 5 shows plots of $|\epsilon_d|$ versus π of surfactant of day 136, thus related to the π-A plot of Fig. 4. Each point represents the mean value of four measurements on two monolayers. The dotted line gives $|\epsilon_d|$ calculated using eqn. (5). The solid curve gives the values calculated using eqns. (6), (7), (9) and (10). We note that the relative difference between the solid and dotted curves decreases with increase of $|\epsilon_d|$.

When we compare this $|\epsilon_d|$-π plot with those of the synthetic compounds discussed in the previous paper (ref.1), we note that this $|\epsilon_d|$-π plot is also similar to that of mixed DPPC-DOPG. $|\epsilon_d|$ increases monotonously to a mean maximum value of $104 mNm^{-1}$, although not so linearly as the synthetics (ref.1). As with the synthetic compounds, ϕ_ϵ was found to differ only slightly from zero $\varphi_\epsilon < 10^o$ which might not be significant. Only in collapse, ϕ_ϵ could attain values up to about 50^o.

Figure 6 shows single measured values of $|\epsilon_d|$ from different days, calculated according to eqns. (6), (7), (9) and (10). Fig. 6a gives $|\epsilon_d|$-π of

five monolayers prepared from days 130-134 and Fig.6b from days 137-140. We note that within the experimental error $|\epsilon_d|$ does not decrease with gestational age after about day 133, as has been reported for the case of crude foetal sheep by Snik et al. (ref.13). This absence of a significant

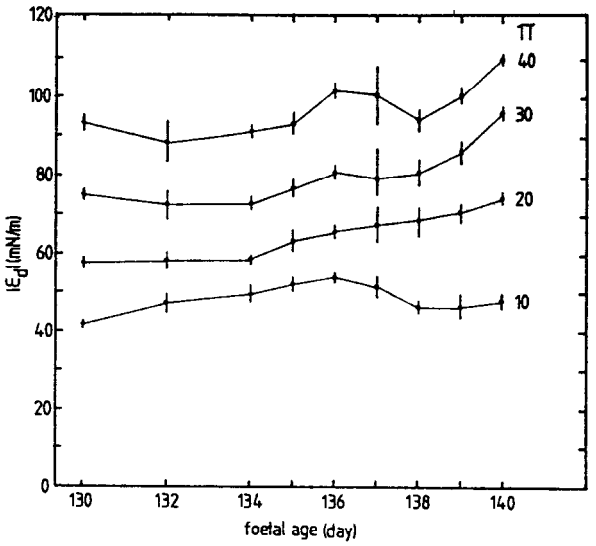

Fig. 7. Plot of $|\epsilon_d|$ vs foetal age at different values of π. End of gestation at the 142th day. Points represent means of two measurements in duplicate on two monolayers and vertical bars range between minima and maxima.

change is also shown in Fig. 7 which represents $|\epsilon_d|$ vs foetal age from days 130 to 140, with π as a parameter (π=10, 20, 30 and 40mNm^{-1}).

Discussion

The result is that fluid monolayers of the phospholipid fraction of foetal surfactant do not show a transition from the liquid-expanded to the liquid-condensed phase. Their π_{max} values are approximately 48mNm^{-1}. The main result is that we found no decrease of $|\epsilon_d|$ with foetal age, as has been reported by Snik et al. (ref.13) in the case of crude foetal lung surfactant. Moreover, a large and significant variation of $|\epsilon_d|$ with foetal age is not at all likely. On the one hand this result is surprising, since it has been fairly generally assumed that foetal surfactant should develop towards maturity at end of gestation. On the other hand however, our findings are in agreement with the lack of variation of the chemical composition with foetal age of the purified foetal sheep surfactant from days 125 to 143 (ref.14).

REFERENCES

1 A.A.H. Boonman, P.M.C. Gieles, C.H. Massen and J. Egberts, Dynamic surface tension measurements on surface active material, Thermochimica Acta, 103 (1986) 107-112.
2 P.M.C. Gieles, Methods of measurement for the evaluation of monolayer properties, thesis, Eindhoven, 1987.
3 A.F.M. Snik, Study of physical properties of monolayers, applications to physiology, thesis, Eindhoven, 1983.
4 E.H. Lucassen-Reynders and J. Lucassen, Properties of capillary waves, Advan. Colloid Interface Sci., 2 (1969) 347-395.
5 J. Lucassen and M. van den Tempel, Dynamic measurements of dilational properties of a liquid interface, Chem. Eng. Sci., 27 (1972) 1283-1291.
6 J. Lucassen and G.T. Barnes, Propagation of surface tension changes over a surface with limited area, J. Chem. Soc., Faraday Trans. 68 (1972) 2129-2138.
7 M. Hallman and L. Gluck, Formation of acidic phospholipids in rabbit lung during perinatal development, Pediatr. Res., 14 (1980) 1250-1259.
8 M. Oulton, A.E. Bent, J.H. Cray, E.R. Luther and L.J. Peddle, Assessment of fetal lung maturity by phospholipid analysis of amniotic fluid lamellar bodies, Am. J. Obstet. Gynecol., 142 (1982) 684-691.
9 B.J. Benson, J.A. Kitterman, J.A. Clements, E.J. Mescher, and W.H. Tooley, Changes in phospholipid composition of lung surfactant during developent in the fetal lamb, Biochim. Biophys. Acta, 753 (1983) 83-88.
10 F. Possmayer, Biochemistry of pulmonary surfactant during fetal development and in the perinatal period, in: B. Robertson, L.M.G. van Golde and J.J. Batenburg (Eds.), Pulmonary surfactant, Elsevier, Amsterdam, 1984.
11 J. Egberts and W.A. Noort, Gestational age-dependent changes in plasma inositol levels and surfactant composition in the fetal rat, Pediatr. Res., 20 (1986) 24-27.
12 A. Beintema-Dubbeldam, J. Bennebroek-Gravenhorst and J. Egberts, Determination of lamellar body phospholipids in amniotic fluid: a method to predict when the fetal lung becomes mature, Gynecol. Obstet. Invest., 21 (1986) 64-69.
13 A.F.M. Snik, A.A.H. Boonman, P.M.C.Gieles and J. Egberts, Viscoelastic properties of lung surfactant, Prog. Resp. Res., 18 (1984) 24-28.
14 J. Egberts, G.C.M. Corree and A.A.H. Boonman, Lack of change in the composition of fetal lamb lung surfactant during gestation, Biochim. Biophys. Acta, 878 (1986) 146-151.